

Tandem mass spectrometry and multiple reaction monitoring using an atmospheric pressure chemical ionization triple quadrupole mass spectrometer for product identification in atmospherically important reactions

Janeen Auld and Donald R. Hastie (corresponding author)

Department of Chemistry and The Centre for Atmospheric Chemistry, York University, 4700 Keele St, Toronto, Ontario, M3J 1P3, Canada. E-mail [Hastie@Yorku.ca](mailto:Hastie@Yorku.ca) Telephone 1-416-736-5410 Fax 1-416-736-5411

## Abstract

An atmospheric pressure chemical ionization triple quadrupole mass spectrometer has been coupled to a smog chamber to study the products of atmospherically important hydrocarbon oxidation reactions. Traditional MS and MS/MS scan modes were used to identify ion signals arising from possible reaction products and Multiple Reaction Monitoring (MRM) was used to follow a number of these as target→fragment ion pairs over the course of the reaction.

Mechanistic information has been inferred from the time dependence of product signals. MRM profiling has allowed identification of interferences that occur due to isobaric ions resulting from the formation of isobaric products and/or clustering, which can be undetectable using the MS and MS/MS modes. Differences in product formation rate results in variations of their MRM ion pair onset and time profile therefore allowing separation to be observed. This method was tested during a study of the products of the HO radical oxidation of  $\beta$ -pinene. The oxidation product pinaketone (MW 138) has been shown to have interferences at its  $(M + H)^+$ ,  $m/z$  139, being more accurately monitored using its  $(M + H + H_2O)^+$  cluster ion pairs,  $157 \rightarrow 139$  and  $157 \rightarrow 121$ . Furthermore, the time dependence of the ion pair  $157 \rightarrow 111$  has led to identification of a more highly oxidized acid-aldehyde product. It has been determined that an organic nitrate contributing to  $m/z$  216 based on its time dependence relative to pinaketone cannot be the expected simple C<sub>10</sub> hydroxynitrate product but rather a more highly oxidized C<sub>9</sub> nitrate. Using

MRM to follow ion signals as a function of reaction time has proven to be a valuable addition to existing mass spectrometric acquisition modes for reaction product determination.

*Keywords:* mass spectrometry, atmospheric pressure chemical ionization,  $\beta$ -pinene, oxidation

## **1. Introduction**

Studies of tropospheric chemistry deal mainly with the reactions of compounds emitted from natural and anthropogenic sources [1], [2]. These reactions serve to cleanse the atmosphere of these low oxidation state species through the production of oxidants such as ozone, and provide a mechanism for the atmosphere to move towards thermodynamic equilibrium. When these reactions involve only naturally occurring compounds at natural levels they maintain steady state concentrations of trace gases and particulate matter and the oxidation state of the atmosphere; however since the industrial revolution natural emissions have been supplemented by anthropogenic emissions. These can significantly enhance the natural chemistry by increasing the concentration of the naturally occurring compounds or by adding new, and frequently more reactive, compounds to the atmosphere. The result of this enhanced chemistry is seen in most highly populated and industrialized areas in the form of “smog” characterized by high oxidant (e.g. O<sub>3</sub> and PAN) levels and the presence of elevated levels of fine particulate matter. There is unequivocal evidence that these high oxidant levels have negative impacts on human health and plant productivity [3] and particulate matter is strongly associated with increased respiratory and cardiovascular impacts on human health [4].

Hydrocarbons are emitted in very large quantities from both natural and anthropogenic sources and have been identified as one of the most important classes of reactive compounds producing high oxidant levels and particulate matter [5], [6]. The oxidation of these compounds involves

multi-step reactions that produce ozone, recycle hydroxyl radicals and, for larger molecules, contribute significantly to the production of secondary particulate matter [7], [8]. Knowledge of the rates and products of these oxidations are essential for the successful implementation of this chemistry into atmospheric models that can be used as the basis of control strategies for air quality improvement.

The reaction rate constants for the initial attack on most of the atmospherically important hydrocarbons have been determined [9]. Techniques exist for determining rate constants for reactions with the most common atmospheric oxidants: Ozone  $O_3$ ; the hydroxyl radical HO; and the nitrate radical  $NO_3$  often by measuring the decay of both the reagent and the oxidant. The oxidation products of the simple hydrocarbons have been determined but are, for the most part, lacking for the larger hydrocarbons. Generally the reaction pathways to products are constructed based on our knowledge of the pathways for the simpler molecules [10]. This methodology becomes incomplete for larger systems where isomerization and cyclizations that cannot occur in the smaller molecules become possible [11]. The lack of detailed reaction product information manifests itself in a number of problems in using atmospheric chemistry models for environmental prediction. The products of hydrocarbon oxidation are themselves reactive hydrocarbons and will undergo further oxidation. Without a full knowledge of their identity and oxidation chemistry the mechanisms in the models are incomplete. Larger hydrocarbons produce low vapour pressure products that can partition into the particulate phase. The contribution of this secondary organic matter to the total particulate matter burden can be significant. In urban areas organics contribute 20-50% of the total particulate mass with most of this resulting from the reactions of gas phase hydrocarbons, with even higher fractions in heavily forested areas [12]. Improving the predictive ability of air quality models for oxidants and particulate matter requires complete information on the identity, reactivity, and vapour pressures of the products of hydrocarbon oxidation.

Identification of reaction products is a challenge because, unlike kinetic studies, the nature of the target molecule is not known. This is the opposite problem to most analytical chemistry where methods are tuned to particular species or functional groups so these methods are limited in their utility in determining the unknown products of gas phase reactions. A number of trace gas analytical methods have been successfully applied to the measurement of targeted reaction products. Of these the gas chromatographic (GC) or liquid chromatographic (LC) methods are the most widespread, and those utilizing mass spectrometric (MS) methods have been the most productive for both gas and particulate phase products. Larsen et al. [13] used LC/MS to analyse filter samples from chamber reactions of HO with terpenes. They were able to identify a number of multifunctional oxidation products including dicarboxylic acids, keto carboxylic acids, hydroxy keto carboxylic acids, keto aldehydes, hydroxyl ketoaldehydes, and hydroxyl ketones. They also derivatized carboxylic acid groups and performed GC/MS analysis. Orlando et al. [14] also used GC with flame ionization detection (GC/FID) to follow acetone production from similar systems. Yu et al. [15], [16] derivatized filter samples to convert carbonyls to oxime derivatives and hydroxyl groups in acids and alcohols to trimethylsilyls and used GC/MS to identify a number of hydroxyl and carbonyl containing compounds. These off-line analyses have very good sensitivity but the long collection times necessary to obtain sufficient sample result in very poor time resolution. Consequently, any information on the sequence of product formation is lost. Furthermore since the sample must be collected and undergo some level of preparation prior to analysis, highly reactive species are likely to suffer degradation through this process.

Online methods promise better time resolution and less opportunity for sample degradation. Of these Fourier Transform Infrared Spectroscopy (FTIR) and MS methods are the most widely used. The FTIR methods are limited by spectroscopic constraints so they can identify small molecules but for larger molecules they can only be used to characterize functional groups,

unless the matrix is extremely clean. In addition to their chromatographic measurements Larsen et al. [13] used FTIR to follow gas phase products in real time. Products were assigned using authentic standards but were limited to the major ketone product, acetone, formaldehyde and formic acid. Similarly Orlando et al. [14] and Winterhalter et al. [17] have identified ketones, formaldehyde and formic acid in analogous systems.

MS methods can potentially be applied to a wider range of compounds although tandem mass spectrometry (MS/MS) methods are necessary to obtain sufficient information for product identification. An atmospheric pressure chemical ionization (APCI) MS/MS system is particularly attractive for the identification of gas phase reaction products. This is a comparatively benign ionization compared to most methods so there is much less fragmentation of the target species. This results in a simpler mass spectrum, which is particularly advantageous in sampling complex matrices of compounds. Once ions are produced the MS/MS system can be used to select and fragment a target ion to produce a mass spectrum of its fragment ions. The mass to charge ratio ( $m/z$ ) of the fragments can be used to help elucidate the structure of the target ion. Also the fragment ion spectrum can be used to identify and separate ions with different structures but the same target  $m/z$  (isobaric ions). The complete analysis procedure can be done on-line without pre-treatment of the sample with less than  $1 \text{ L min}^{-1}$  of the sample gas, making this one of the most attractive multispecies methods available.

APCI triple quadrupole [18] and APCI ion trap [19] instrumentation has been used to identify reaction products and monitor their evolution with time. In these applications the reaction product time evolution profiles were generated by monitoring the signal of the target ion,  $(M+H)^+$  and identification of the reaction product was completed using the fragmentations observed under  $MS^n$  conditions (where  $n = 1, 2$  or  $3$ ). MS/MS fragmentation of ions associated with the target ions such as cluster ions were also used to support identifications. Identification of products using only  $MS^n$  fragmentation is very challenging for these reaction systems and

measurement technique considering the potential for formation of isobaric products and therefore ions, additional isobaric ions due to clustering and the fact that the majority of oxidation products are not commercially available or easily synthesized. The latter is a significant hurdle for correctly identifying a single product based on MS<sup>n</sup> spectra.

In this paper we utilize several scan modes of an APCI triple quadrupole system in combination with the time dependence of the reaction product signal to analyze products of hydrocarbon oxidation. Results indicate extending the above methodologies to include MS/MS based time evolution profiles is effective in allowing separation and identification of isobaric ions. We use an unmodified Sciex TAGA 6000 APCI triple quadrupole mass spectrometer that has been coupled to a smog chamber in which the reaction of  $\beta$ -pinene with HO radicals is being studied. (Figure 1 shows the chemical structure and common names of compounds discussed in the text.) The fast response of this instrument means it is possible to obtain mass spectral information while the reaction is proceeding. This presents an opportunity to not only examine the terminal or most stable reaction products but also the sequence in which multiple products appear in the reaction mixture.

## **2. Experimental**

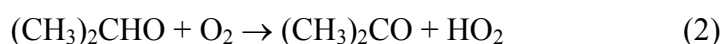
To illustrate the utility of the APCI MS/MS for product identification work we have taken some initial measurements from a study of the HO initiated oxidation of  $\beta$ -pinene in the York University smog chamber.

### *2.1 Smog Chamber*

The chamber is cylindrical in shape with Teflon coated aluminum endplates and transparent Teflon walls. It is  $\sim 8 \text{ m}^3$  in volume and can be irradiated by up to 24 ultraviolet lights (Philips

F40BL, 40 Watt) and has an internal fan to enhance mixing. Prior to each experiment, the chamber was flushed with clean air for at least 24 hours. The reagents  $\beta$ -pinene (Sigma Aldridge), isopropyl nitrite (IPN synthesized in house [20] using isopropyl alcohol in place of n-butyl alcohol) and NO (Air Liquide, diluted 1:100 with nitrogen) were admitted to the chamber and allowed to mix for one hour with the lights off. Typical initial reagent concentrations were: 0.5 ppm  $\beta$ -pinene, 0.4 ppm IPN and 2 ppm NO. Ammonium sulphate ((NH<sub>4</sub>)<sub>2</sub>SO<sub>4</sub>) seed particles of mean diameter 80 nm were added to provide a surface for gas particle partitioning of the reaction products. The seed particles were generated from a  $\sim 0.5 \text{ g L}^{-1}$  (NH<sub>4</sub>)<sub>2</sub>SO<sub>4</sub> solution using a Collison Nebulizer (BGI Inc., Waltham, MA, USA). Measurements of  $\beta$ -pinene, NO gas and particle size distributions were then taken every 5 minutes, as were the mass spectral data. Experiments ran between 1 and 4 hours. Loss of  $\beta$ -pinene in the absence of reaction was negligible implying the chamber walls were inert to this hydrocarbon.

Turning on the lights initiated the chemistry, primarily through the IPN photolysis and HO radical production:



The acetone ((CH<sub>3</sub>)<sub>2</sub>O) produced is less reactive than the expected products of the  $\beta$ -pinene oxidation and so should have limited impact on the reaction system; however it is in high concentrations and was observed to produce clusters with some of the target ions in the MS analysis (see below). Nitric oxide is added to ensure reaction 3 rapidly converts HO<sub>2</sub> to HO, and to limit the accumulation of ozone from the photolysis of NO<sub>2</sub> through reaction 6:



## 2.2 Instrumentation

### 2.2.1 APCI Triple Quadrupole Mass Spectrometer

The mass spectrometer used in this work is a Sciex TAGA 6000E APCI triple quadrupole mass spectrometer (MDS Sciex, Concord, ON, CA) [21]. The reaction mixture is sampled from the smog chamber into the APCI source through 0.64 cm Teflon tubing at a flow rate of  $\sim 2 \text{ L min}^{-1}$ . A 25 mm diameter quartz fibre filter (PALLflex\* Tissuquartz\*, PALL (Canada) Ltd., Toronto, ON, CA) was placed in line prior to the source to isolate the gas phase by removing the particulate in the sample. The sample line is approximately 3.2 m long and attaches to a  $\sim 2$  cm diameter glass tube feeding directly into the source. Air from an Aadco pure air generator (Advanced Analytical Device Company, Cleves, OH, USA) is introduced through a perpendicular inlet in the glass tube to dilute the sample and obtain an optimal flow for the ion source,  $5 \text{ L min}^{-1}$ . The output of the glass tube into the source region is aligned to bring the sample directly into the region between the corona discharge needle and the mass spectrometer sampling orifice.

Since the ionization takes place in air, under the positive conditions used, the corona discharge produces  $\text{N}_2^+$  and  $\text{O}_2^+$  which subsequently react with water vapour to produce intermediate ions ( $\text{H}_3\text{O}^+(\text{H}_2\text{O})_n$ ,  $n=0,1,2,\dots$ ). For most hydrocarbons the proton affinity is greater than that of the hydrated hydronium ion so proton transfer is energetically favoured to produce an ion of molar mass plus 1 amu ( $\text{M}+\text{H}^+$ ). For hydrocarbons with much lower proton affinities charge transfer to



produce a true molecular ion ( $M^+$ ) is possible. Thus the APCI source produces  $M^+$  or  $(M+H)^+$  ions in high numbers with limited fragmentation. The ions are drawn from the source region into the analyzer region through a nitrogen curtain gas by a potential drop of 610V between the interface plate and orifice ring.

The high pressure of the APCI source allows a number of ion molecule reactions to produce higher  $m/z$  ions of the form  $(M + H + (H_2O)_n)^+$  [22], [23] and  $(M_1 + H + M_2)^+$  where  $M_1$  and  $M_2$  may be the same or different species. The most prominent form of the latter cluster involves the highly abundant acetone with other products.

### *2.2.2 Ancillary monitors*

The concentration of the hydrocarbon was followed by GC/FID using a Hewlett Packard 5890 Gas Chromatograph, equipped with a non-polar Supelco SPB-1 capillary column (30 m x 0.53 mm x 0.5  $\mu$ m film). This instrument was calibrated against standards generated by diluting the emission from a temperature controlled permeation tube (VICI Valco Instruments Co. Inc.) calibrated by weight loss. A chemiluminescence  $NO_x$  Analyser (TE Inc. Model 42S) calibrated against a certified standard mixture of NO in  $N_2$  (Air Liquide) was used to measure NO concentrations.

### *2.3 Operation of the mass spectrometer*

This instrument was used in three modes.

In the MS mode the mass spectrum of all the ions is generated. This spectrum is used for the preliminary identification of molecular and cluster species. In the MS/MS mode a single target ion is selected in the first quadrupole. It is then injected into the second quadrupole at a known and controllable energy. This quadrupole contains argon at comparatively high pressure so that

the target ion can be fragmented through collisions with the neutral molecules. The ionic fragments are analyzed by the third quadrupole. Examination of these fragment ions gives structural information on the target ion and so allows more definitive assignment of the peaks in the MS spectrum. Further refinement is possible by controlling the energy imparted to the ions prior to entering the collision cell. For example stronger bonds require higher collision energies to produce characteristic fragments of this bond cleavage.

In this paper we accentuate the use of the Multiple Reaction Monitoring (MRM) (also known as Selected Reaction Monitoring (SRM)) [24] for elucidating some features of the reaction system. In MRM a specific fragment ion (F) is identified from the MS/MS spectrum of a target ion (T). By setting the first quadrupole to only pass ion T and the third quadrupole to only pass ion F, a highly specific and possibly unique molecular identification is possible. It is the unique identification that is the basis of most MRM applications in analytical science. Typically when a known compound is being quantified, say by LC-MS, a unique target fragment ion pair  $T \rightarrow F$  is identified through the use of authentic standards and this fragment is monitored to give quantitative information on the concentrations in a sample. By spending analysis time only on the targeted ion pairs the signal to noise performance, compared to the MS/MS mode, is greatly improved. Using a  $T \rightarrow F$  ion pair for a reaction product under study reduces the scanning time associated with each reaction product increasing the efficiency of the method allowing a larger number of products to be monitored as the reaction proceeds. Isobaric products form through different oxidation pathways and therefore different rates, which can be identified using the MRM evolution profiles. Further coupling of these data, for many products, with an understanding of possible reaction pathways can improve our understanding of the reaction system.

### 3. Results: Use of APCI-MS/MS in elucidating reaction products and mechanisms

#### 3.1 Product identification from MS/MS spectra

An expected product of the  $\beta$ -pinene oxidation is pinaketone (Fig. 1), which has a molar mass of 138 and should ionize by proton transfer to give the protonated molecular ion at  $m/z$  139. Fig. 2a. shows the MS/MS spectrum of  $m/z$  139 from the reaction mixture. On collision this target ion shows reasonable losses for a ketone namely 18 amu ( $H_2O$ ), 46 amu ( $C_2H_6O$ ), and 56 amu ( $C_3H_4O$ ) to give ions containing no oxygen at  $m/z$  121 ( $C_9H_{13}$ ),  $m/z$  93 ( $C_7H_9$ ), and  $m/z$  83 ( $C_6H_{11}$ ), respectively. Below  $m/z$  97 the typical hydrocarbon signature of mass differences of 14 amu ( $CH_2$ ) are prevalent.

In a case such as this, where the MS/MS spectrum strongly suggests a stable compound that is available, or can be synthesized, it can be positively identified as a reaction product by comparison of its MS/MS spectrum with an authentic sample of the pure compound. In Fig. 2b, an MS/MS spectrum of  $m/z$  139 from pinaketone is shown. The correspondence in both the  $m/z$  of the fragment ions and their relative peak intensities in the spectra in Fig. 2 positively identifies the presence of pinaketone in the reaction mixture. In addition there is no evidence in the  $m/z$  139 reaction sample MS/MS spectra to suggest the presence of contributions from species other than pinaketone at  $m/z$  139.

#### 3.2 Use of MRM to identify reaction products contributing to the same mass peaks

In these experiments, pinaketone is expected to be oxidized and produce multifunctional acids, aldehydes, and ketones. In this method the search for oxidation products is complicated by ion molecule reactions in the ionization region that result in the formation of product clusters to water and other products as mentioned earlier. These clusters can be challenging to distinguish from products since they will produce fragments such as a loss of water, which is a characteristic

loss of oxidation products containing hydroxy and carbonyl moieties. Additionally, potential products could be overlooked if they have the same  $m/z$  ratio as a cluster of a known compound. Pinaketone appears in the MS mode as an  $(M+H)^+$  peak at  $m/z$  139, and would reasonably be expected to also form a water cluster at  $m/z$  157. The low collision energy MS/MS spectra of  $m/z$  157 from a sample of pure pinaketone in Fig. 3 shows this ion easily dissociates into the same  $m/z$  139,  $m/z$  121 and  $m/z$  83 ions of pinaketone itself, confirming this assignment. No other significant fragment ions are seen because of the low collision energy used. We chose to use MRM to follow the pinaketone and its water cluster target ions through their fragment ion at 121, which is the hydrocarbon backbone  $C_9H_{12}$ . These MRM signals as a function of reaction time are shown in Fig. 4. Both  $m/z$  139 $\rightarrow$ 121 and  $m/z$  157 $\rightarrow$ 121 show some signal prior to the  $\beta$ -pinene oxidation commencing at time  $t=0$ . This is due to the ubiquitous presence of pinaketone in commercially available  $\beta$ -pinene.

Following the onset of the  $\beta$ -pinene oxidation, it is clear that these signals do not represent the same species, or at least not exclusively the same species. At short reaction times the profiles show the same time for the onset of the increase expected as pinaketone is produced. However, as the reaction proceeds, the signals diverge. Especially notable is the almost constant  $m/z$  139 $\rightarrow$ 121 signal after 30 minutes, suggesting the product does not react further. This is inconsistent with the expected behaviour of pinaketone which would be expected to undergo further oxidation as the rate constant for the HO radical reaction with pinaketone is 20% that for  $\beta$ -pinene.

The target fragment pair for the proposed water cluster at  $m/z$  157 $\rightarrow$ 121 behaves as would more reasonably be expected of a marker of pinaketone. It rises rapidly following the onset of reaction and decays as would be expected for a product undergoing further reaction. However, at longer times ( $>100$  min) the signal reaches a steady value suggesting that either the product is no longer reacting due to other insufficient reagents or that another product occurring late in the

reaction sequence also has a contribution to  $m/z$  157→121. The combination of the MS/MS, MRM and an understanding of the expected chemistry suggests that, in the first hour and a half of the experiment, pinaketone is better followed using the target fragment pair of  $m/z$  157→121 rather than the more intuitive  $m/z$  139→121, but that there may be an additional product contributing significantly to this pair at longer times.

If  $m/z$  157→121 represents the pinaketone, the question remains how to explain the apparently constant  $m/z$  139→121 signal. This could be explained by the appearance of an additional contribution to the signal following the maximum in the pinaketone concentration. This contribution could come from another product with the same  $(M+H)^+$  at  $m/z$  139 or from a larger ion that produces a fragment ion of  $m/z$  139 in the ion source. While it is expected, and has been shown above, that pinaketone  $(M+H)^+$  clusters to water, it is also reasonable to consider that there may also be a product at  $m/z$  157. The MS/MS spectrum of  $m/z$  157 from the reaction mixture taken at  $t = 48$  min, in Fig. 5., shows the same  $m/z$  139 and  $m/z$  121 peaks as the pure pinaketone standard for the same collision energy. However the comparison reveals a unique fragment peak at  $m/z$  111, a loss of 46 amu from  $m/z$  157 that is not present in the MS/MS spectrum of the standard. The reaction mixture MS/MS therefore points to the presence of an additional product contributing to  $m/z$  157.

Following the time evolution of this additional species can tell us more about its possible identity and possible precursors. In the MRM experiments we followed the  $m/z$  157→111 ion pair through the reaction, and this is plotted along with  $m/z$  139→121 and  $m/z$  157→121 in Fig. 6. Unlike the previously identified pinaketone related ions, there is no signal from this ion pair prior to the onset of the reaction. The product generating the target fragment ion pair at  $m/z$  157→111 has a markedly different time evolution to the  $m/z$  157→121. It appears 35 minutes into the reaction, much later than the pinaketone, and has a much slower decay after reaching its maximum. The late appearance would suggest it is a more highly oxidized species than

pinaketone that is likely being formed from  $\beta$ -pinene in two or more oxidation steps and its slow decay indicates it is somewhat less reactive than pinaketone. A previously identified product, with the correct molecular weight, that meets these criteria and so would be a reasonable candidate for this product is the acid-aldehyde, norpinalic acid ( $C_8H_{12}O_3$ , Fig. 1) [13]. Furthermore, this product could also contribute to the observed  $m/z$  139 signal through fragmentation in the ion source losing a neutral of 18 amu. Such source fragmentation is possible in the APCI source even though the energy involved is relatively low [21]. In the MS/MS or MRM modes this  $m/z$  139 ion would lose another 18 amu to give a contribution to the  $m/z$  139 $\rightarrow$ 121 profile. Therefore this newly identified product can be seen through its fragmentations  $m/z$  157 $\rightarrow$ 111 but would probably also contribute to the  $m/z$  139 $\rightarrow$ 121 signal, preventing its use as an effective target for pinaketone.

Comparing the profiles in Fig. 6 it is observed that  $m/z$  157 $\rightarrow$ 121 begins to decline at  $t=30-35$  mins which correlates to the onset of  $m/z$  157 $\rightarrow$ 111. If in fact  $m/z$  139 $\rightarrow$ 121 is composed of contributions from pinaketone and the  $m/z$  157 product identified at  $m/z$  157 $\rightarrow$ 111 then the difference between  $m/z$  139 $\rightarrow$ 121 and  $m/z$  157 $\rightarrow$ 111 should match the observed profile of  $m/z$  157 $\rightarrow$ 121. This difference is shown in Fig. 7, with no attempt to allow for possible instrumental sensitivity differences between the species included. The difference correlates much better to the observed decay of  $m/z$  157 $\rightarrow$ 121 than did the  $m/z$  139 $\rightarrow$ 121. Although the product represented by  $m/z$  157 $\rightarrow$ 111 appears to be a strong candidate for contribution to the  $m/z$  139 $\rightarrow$ 121 profile there remains an unexplained faster decay in the  $m/z$  157 $\rightarrow$ 121 ion pairs than in the difference profile that drove the search for yet another product contributing to T $\rightarrow$ F 139 $\rightarrow$ 121.

Water is not the only species to form clusters with reaction product ions. In particular the product(s) with molecular weight of 58, expected to be predominantly acetone was found to cluster significantly to the other products formed. A probable pinaketone cluster with acetone

was observed at  $m/z$  197. The lack of losses smaller than 58 amu from the  $(M+H)^+$  in the MS/MS of  $m/z$  197 in Fig. 8 and the appearance of the same fragment ions as  $m/z$  139 strongly suggests this is a cluster of pinaketone. The MRM profiles as a function of reaction time for  $m/z$  139 $\rightarrow$ 121,  $m/z$  157 $\rightarrow$ 121 and  $m/z$  197 $\rightarrow$ 121 are shown in Fig. 9a. All three profiles indicate products at the same time however the signal at  $m/z$  197 $\rightarrow$ 121 rises to a constant value much more slowly than the other two ion pairs. This indicates another product, either partly or fully, contributing to the  $m/z$  197 $\rightarrow$ 121 signal. In this case there is no identifiable unique fragment ion in the  $m/z$  197 MS/MS that can be used to confirm this assignment. Even though the identity of this species is not known at this time the potential for contribution to the  $m/z$  139 $\rightarrow$ 121 profile is reasonable through source fragmentation of the  $m/z$  197 ion resulting in a loss of 58 amu to produce the  $m/z$  139 ion. Subsequent loss of 18 amu from the  $m/z$  139 source fragment ion is also reasonable given the highly oxidized nature necessary for a product of this mass. If we assume that the contributions to the  $m/z$  197 $\rightarrow$ 139 and  $m/z$  197 $\rightarrow$ 121 profiles are dominantly from the product at  $m/z$  197 one would expect that subtracting both the  $m/z$  157 $\rightarrow$ 111 and  $m/z$  197 $\rightarrow$ 121 profiles from the  $m/z$  139 $\rightarrow$ 121 profile would result in a more accurate pinaketone profile that should match well with  $m/z$  157 $\rightarrow$ 121. Fig. 9b shows that including  $m/z$  197 $\rightarrow$ 121 does in fact improve the correlation of  $m/z$  139 $\rightarrow$ 121 to  $m/z$  157 $\rightarrow$ 121 providing further evidence for  $m/z$  157 $\rightarrow$ 121 being the best available indicator for pinaketone in the early stages of the reaction.

Hence the application of MS/MS to this system has identified pinaketone as a product of the reaction, both through its  $(M+H)^+$  ion and its cluster with water. Combination with MRM as a function of reaction time has illustrated the existence and ability to separate isobaric ions as well as providing additional information regarding the identity of products.

### *3.3 Identification of organic nitrates.*

Current understanding of the oxidation chemistry of  $\beta$ -pinene suggests that radical attack on the hydrocarbon is followed by addition of oxygen to produce peroxy radicals. Under the high  $\text{NO}_x$  conditions used in this study these radicals can react with NO through two channels to give either the alkoxy radical or the organic nitrate. As the pathway to form nitrates is more favoured for larger alkyl groups [1] organic nitrates should be a significant product in the experiments reported here.

Provided it is an  $(\text{M}+\text{H})^+$  mass peak,  $m/z$  216 could be an organic nitrate as its even mass implies it contains a single nitrogen atom. The MS/MS spectrum of  $m/z$  216 from the reaction is shown in Fig. 10. Most of the peaks are typical of oxygenated nitrates:  $m/z$  198 (loss of 18 amu ( $\text{H}_2\text{O}$ )),  $m/z$  170 (loss of 46 amu ( $\text{NO}_2$  or  $\text{H}_2\text{O}$  and  $\text{CO}$ )), and  $m/z$  152 (loss of 64 amu ( $\text{H}_2\text{O}$  and  $\text{NO}_2$  or  $2\text{H}_2\text{O}$  and  $\text{CO}$ )). The fragment ion observed at  $m/z$  158 has been shown to be unrelated to the rest of the fragment ions and is due to a cluster of another product. Addition of a single nitrate group is insufficient to account for the mass of this product being 79 amu higher than the  $\beta$ -pinene, so this molecule must be a di- or more highly substituted product. Aschmann et al. [18] have suggested that this product is most likely a hydroxynitrate of the  $\beta$ -pinene backbone ( $\text{C}_{10}\text{H}_{17}\text{NO}_4$ , Fig. 1). This is consistent with known mechanisms where HO radical attack on the exocyclic double bond followed by NO addition to the peroxyradical would result in an  $\alpha$ -hydroxynitrate. Alternative non-trivial isomeric structures must include higher oxidation products involving the loss of the exocyclic methylene to give a  $\text{C}_9\text{H}_{13}\text{NO}_5$  compound such as a bicyclic hydroxy-oxo-nitrate or a monocyclic dicarbonyl-nitrate (Fig. 1). At the level of resolution available with this instrument further distinction between the isomers is not possible. However since the production of the  $\text{C}_9$  isomers require multiple reaction steps, monitoring the appearance of products by MRM can give vital mechanistic information. Fig. 11 shows the MRM profile of  $m/z$  216 $\rightarrow$ 152 for the nitrate along with the pinaketone at  $m/z$  157 $\rightarrow$ 121 as a function of reaction time. If this product is the  $\alpha$ -hydroxynitrate it should be produced very



early in the reaction sequence and mimic the production of pinaketone that results from the peroxy radical channel. However, the  $m/z$  216 product is formed substantially after the production of pinaketone at a time similar to that of the proposed norpinalic acid above. This suggests that the bulk of the  $m/z$  216 observed here is not the  $\alpha$ -hydroxynitrate but a product that is produced late in the reaction mechanism consistent with the  $C_9$  nitrates. The exact identification of this nitrate and the details of its formation mechanism remain to be clarified. It is clear that the additional information provided by the MRM profiles as a function of reaction time is valuable in clarifying details of nitrate products and their production pathways.

#### 4. Conclusion

Monitoring a reacting system in real time using MS/MS has been shown to provide valuable information on the identity of the reaction products and their time evolution can yield insights into the dominant reaction pathways. Following the gas phase oxidation of  $\beta$ -pinene by HO radicals using an APCI triple quadrupole MS system was used as an example. MS mode spectra can point to products but to clarify the multiple products from large molecules, particularly those of successive reactions, MS/MS capability is essential. In this example the product pinaketone was postulated based on the MS/MS spectra of its protonated parent ion at  $m/z$  139 and its water cluster at  $m/z$  157. This assignment was confirmed through comparison with the MS/MS spectrum of the pure compound. In the absence of authentic standards the identification cannot be confirmed, as a number of isomers are usually possible, such as the example of the nitrate product with  $m/z$  216.

The use of MRM as a reaction proceeds adds another dimension to the identification of reaction products. Pinaketone was followed through its  $(M+H)^+$  ion at  $m/z$  139 $\rightarrow$ 121 and its water cluster at  $m/z$  157 $\rightarrow$ 121. Variations in the time evolution between these signals indicated the

presence of additional products. One of these products was tentatively identified and in addition its appearance at later reaction times than pinaketone shows it results from secondary or higher order reactions. Similarly the relatively late appearance of the nitrate with  $m/z$  216 eliminates the most obvious possible structure and shows the need for further investigation of the mechanisms for nitrate production.

Thus we have shown that by applying a range of monitoring tools available in a real time MS/MS system can provide the detailed information on reaction products that is invaluable in determining the complete oxidation mechanisms necessary for inclusion in diagnostic and predictive air chemistry models.

### **Acknowledgements**

This work was done with support from the National Sciences and Engineering Research Council of Canada (NSERC), and the Ontario Ministry of the Environment. Contributions from N. Karellas and J. Merritt are gratefully acknowledged.

### **References**

- [1] B.J. Finlayson-Pitts, J.N. Pitts, Chemistry of the upper and lower atmosphere: Theory, experiments and applications, Academic Press, San Diego, CA, 2000.
- [2] J.H. Seinfeld, S.N. Pandis, Atmospheric Chemistry and Physics: From Air Pollution to Climate Change, 2nd ed., Wiley-Interscience, New York, 2006.
- [3] A.S. Lefohn, J.K. Foley, Establishing relevant ozone standards to protect vegetation and human health: Exposure/dose-response considerations, J. Air Waste Manage. Assoc. 43 (1993) 106-112.
- [4] J.L. Mauderly, J.C. Chow, Health effects of organic aerosols, Inhal. Toxicol. 20 (2008) 257-288.

- [5] C.N. Hewitt, Reactive hydrocarbons in the atmosphere, Academic Press, San Diego, 1999, pp. 322.
- [6] R. Koppmann, Volatile organic compounds in the atmosphere, 1st ed., Blackwell Pub., Oxford; Ames, Iowa, 2007.
- [7] J.H. Seinfeld, J.F. Pankow, Organic atmospheric particulate material, *Annu. Rev. Phys. Chem.* 54 (2003) 121-140.
- [8] M.C. Jacobson, H.-C. Hansson, K.J. Noone, R.J. Charlson, Organic atmospheric aerosols: Review and state of the science, *Rev. Geophys.* 38 (2000) 267-294.
- [9] R. Atkinson, J. Arey, Atmospheric degradation of volatile organic compounds, *Chem. Rev.* 103 (2003) 4605-4638.
- [10] A. Calogirou, B.R. Larsen, D. Kotzias, Gas-phase terpene oxidation products: A review, *Atmos. Environ.* 33 (1999) 1423-1439.
- [11] R. Atkinson, Atmospheric chemistry of VOCs and NO<sub>x</sub>, *Atmos. Environ.* 34 (2000) 2063-2101.
- [12] M. Kanakidou, J.H. Seinfeld, S.N. Pandis, I. Barnes, F.J. Dentener, M.C. Facchini et al., Organic aerosol and global climate modelling: A review, *Atmos. Chem. Phys.* 5 (2005) 1053-1123.
- [13] B.R. Larsen, D. DiBella, M. Glasius, R. Winterhalter, N.R. Jensen, J. Hjorth, Gas-phase OH oxidation of monoterpenes: Gaseous and particulate products, *J. Atmos. Chem.* 38 (2001) 231-276.
- [14] J.J. Orlando, B. Noziere, G.S. Tyndall, G.E. Orzechowska, S.E. Paulson, Y. Rudich, Product studies of the OH- and ozone-initiated oxidation of some monoterpenes, *J. Geophys. Res.* 105 (2000) 11561-11572.
- [15] J. Yu, R.C. Flagan, J.H. Seinfeld, Identification of products containing -COOH, -OH, and -C:O in atmospheric oxidation of hydrocarbons, *Env. Sci. and Tech.* 32 (1998) 2357-2370.
- [16] J. Yu, D.R.I. Cocker, R.J. Griffen, R.C. Flagan, J.H. Seinfeld, Gas-phase ozone oxidation of monoterpenes: Gaseous and particulate products, *J. Atmos. Chem.* 34 (1999) 207-258.
- [17] R. Winterhalter, P. Neeb, D. Grossmann, A. Kolloff, O. Horie, G. Moortgat, Products and mechanism of the gas phase reaction of ozone with  $\beta$ -pinene, *J. Atmos. Chem.* 35 (2000) 165-197.
- [18] S.M. Aschmann, A. Reissell, R. Atkinson, J. Arey, Products of the gas phase reactions of the OH radical with  $\alpha$ - and  $\beta$ -pinene in the presence of NO, *J. Geophys. Res. [Atmos.]* 103 (1998) 25553-25561.
- [19] B. Warscheid, T. Hoffmann, On-line measurements of  $\alpha$ -pinene ozonolysis products using an atmospheric pressure chemical ionisation ion-trap mass spectrometer, *Atmos. Environ.* 35 (2001) 2927-2940.
- [20] W.A. Noyes, n-Butyl nitrite, *Organic Syntheses* 16 (1936) 7-8.

[21] P.H. Dawson, J.B. French, J.A. Buckley, D.J. Douglas, D. Simmons, The use of triple quadrupoles for sequential mass spectrometry: 2—A detailed case study, *Org. Mass Spectrom.* 17 (1982) 212-219.

[22] A. Good, D.A. Durden, P. Kebarle, Mechanism and rate constants of ion-molecule reactions leading to formation of  $H^+(H_2O)_n$  in moist oxygen and air, *J. Chem. Phys.* 52 (1970) 222-229.

[23] A. Good, D.A. Durden, P. Kebarle, Ion-molecule reactions in pure nitrogen and nitrogen containing traces of water at total pressures 0.5-4 torr. kinetics of clustering reactions forming  $H^+(H_2O)_n$ , *J. Chem. Phys.* 52 (1970) 212-221.

[24] W.L. Budde, *Analytical mass spectrometry: Strategies for environmental and related applications*, American Chemical Society, Oxford University Press, New York, 2001.

## List of figure captions

Fig. 1. Chemical structures, common names and molecular weights of  $\beta$ -pinene and proposed oxidation products discussed in the text. In cases where multiple isomers are possible, only one is presented.

Fig. 2. Comparison of the MS/MS spectra of target  $m/z$  139 from a) the reaction mixture and b) a pinaketone standard sample. The collision energy for both samples is 10eV.

Fig. 3. MS/MS spectra of target  $m/z$  157 obtained using a pinaketone standard sample at collision energy of 10 eV.

Fig. 4. Reaction time profiles of T→F pairs 139→121 ( $\blacklozenge$ , left axis) and  $m/z$  157→121 ( $\Delta$ , right axis) of pinaketone. The 157→121 profile shows the expected profile of pinaketone with decay due to reactivity to HO radicals. The 139→121 pair is proposed to have contributions from products in addition to pinaketone, see text.

Fig. 5. MS/MS spectra of target  $m/z$  157 acquired 48 minutes after initiating the reaction. The fragment observed at  $m/z$  111 is unique to the reaction mixture MS/MS suggesting the presence of a unique product at  $m/z$  157 in addition to the pinaketone cluster with  $H_3O^+$ .

Fig. 6. Reaction time profiles of T→F pairs  $m/z$  139→121 ( $\blacklozenge$ , left axis),  $m/z$  157→121 ( $\Delta$ , right axis) and  $m/z$  157→111 ( $\square$ , left axis) showing the delayed formation of the unique product at target  $m/z$  157 using T→F pair 157→111.

Fig. 7. Reaction time profiles of T→F pair  $m/z$  157→111 subtracted from  $m/z$  139→121 ( $\times$ , left axis) and  $m/z$  157→121 ( $\Delta$ , right axis). The  $m/z$  139→121 profile has an unexpected plateau for pinaketone, which is known to react with HO radicals. The subtraction of the  $m/z$  157 product contributions to  $m/z$  139→121 results improves the correlation between  $m/z$  139→121 and  $m/z$  157→121.

Fig. 8. Reaction mixture MS/MS spectra of target a)  $m/z$  139 and b)  $m/z$  197. The MS/MS comparison illustrates the consistency of fragments observed for both target ions strongly supporting the identification of target  $m/z$  197 as a cluster of pinaketone.

Fig. 9. Reaction time profiles of a) T→F pairs  $m/z$  139→121 ( $\blacklozenge$ , left axis),  $m/z$  157→121 ( $\Delta$ , right axis) and  $m/z$  197→121 (+, right axis) and b) T→F pairs  $m/z$  139→121 ( $\blacklozenge$ , left axis),  $m/z$  139→121 subtract  $m/z$  157→111 and  $m/z$  197→121 ( $\times$ , left axis) and  $m/z$  157→121 ( $\Delta$ , right axis).

Fig. 10. Reaction mixture MS/MS spectra of target  $m/z$  216 at collision energy of 2eV. The peak at  $m/z$  158 has been found to result from a separate species than the suspected nitrate product.

Fig. 11. Reaction time profile of target  $m/z$  139→121 ( $\blacklozenge$ , left axis) and  $m/z$  216→152 ( $\diamond$ , right axis) illustrating the delayed formation of the product at  $m/z$  216 in comparison to pinaketone.

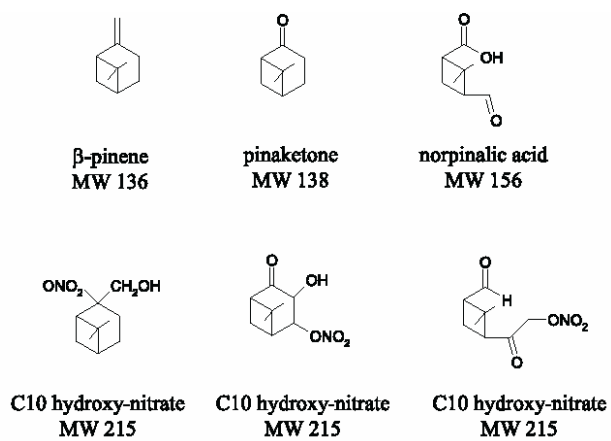


Fig. 1.

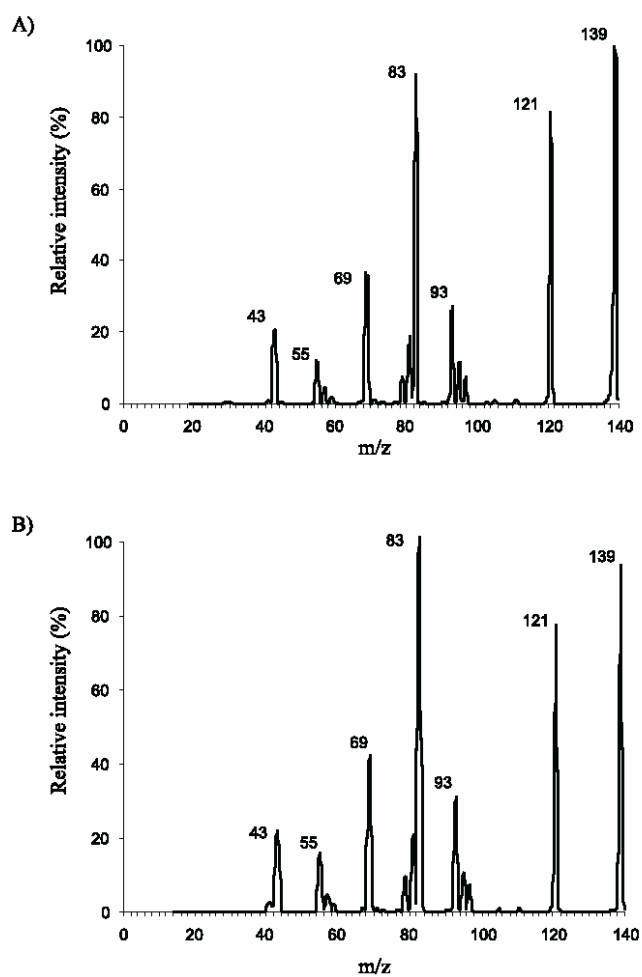


Fig. 2.

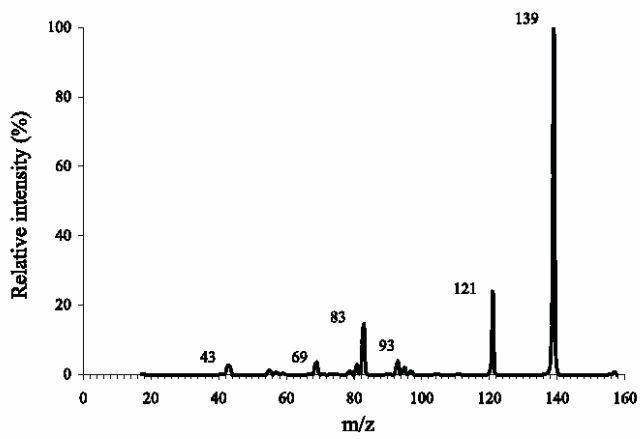


Fig. 3.

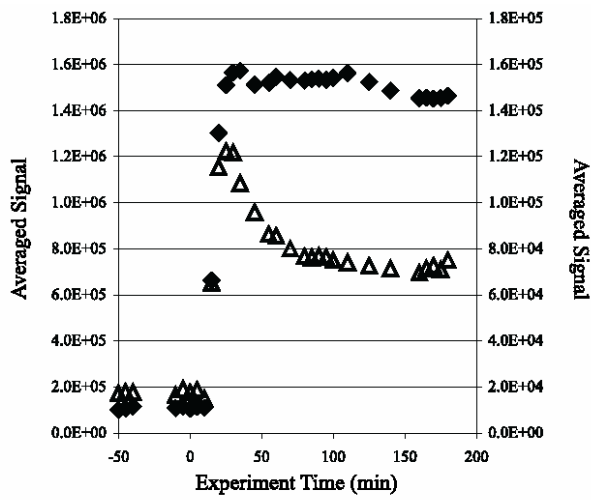


Fig. 4.

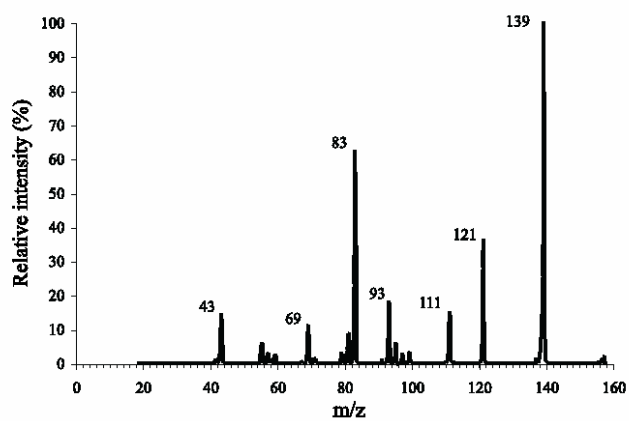


Fig. 5.

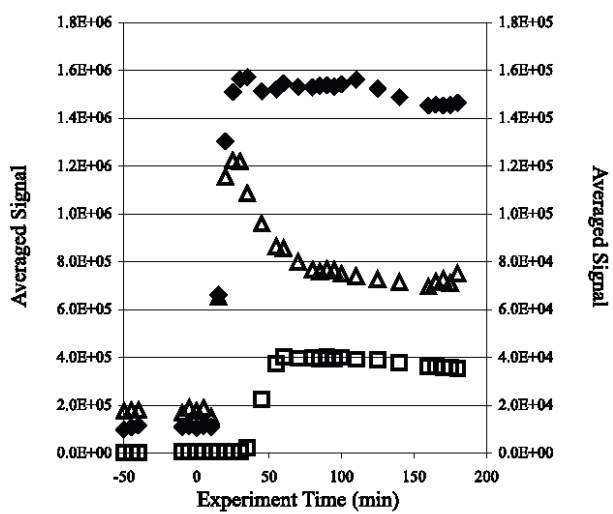


Fig. 6.



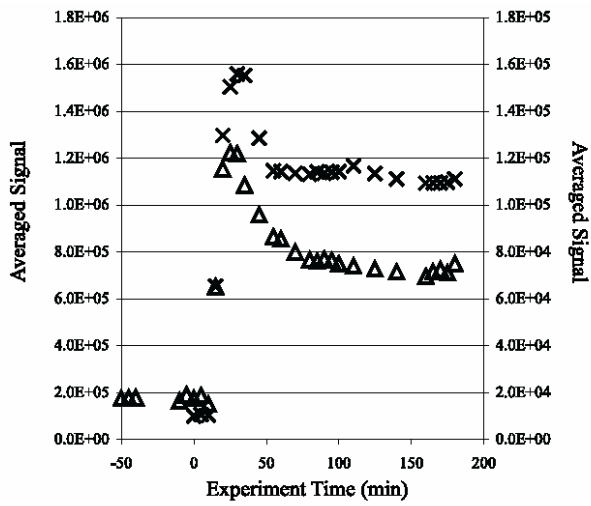


Fig. 7.

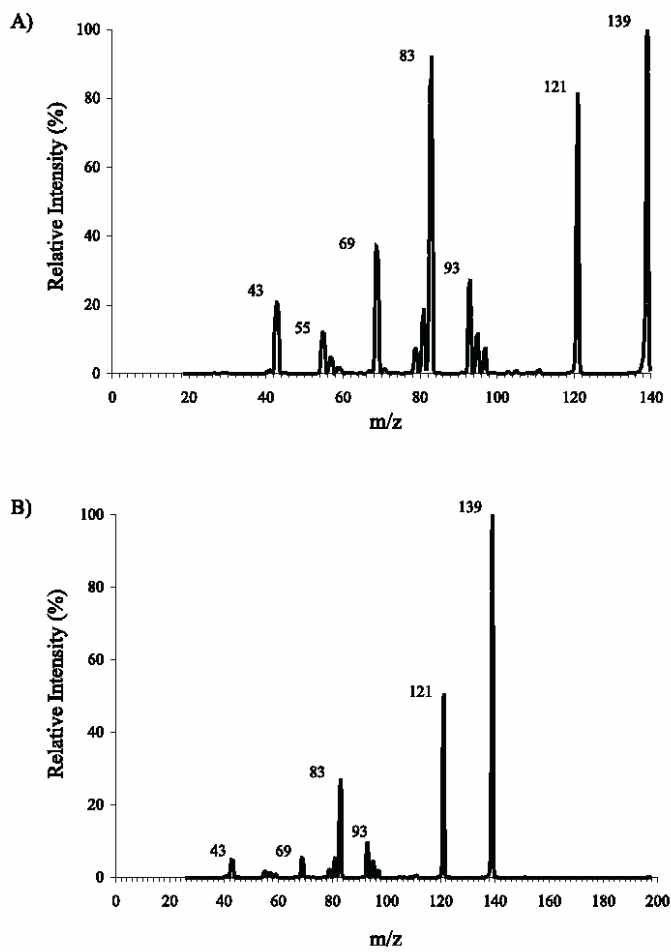


Fig. 8.

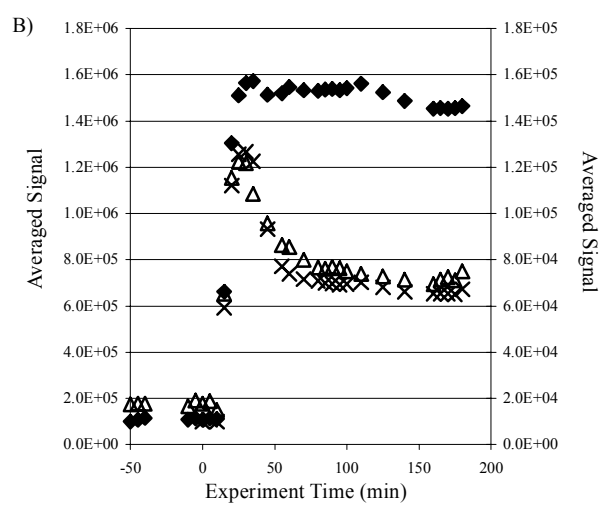
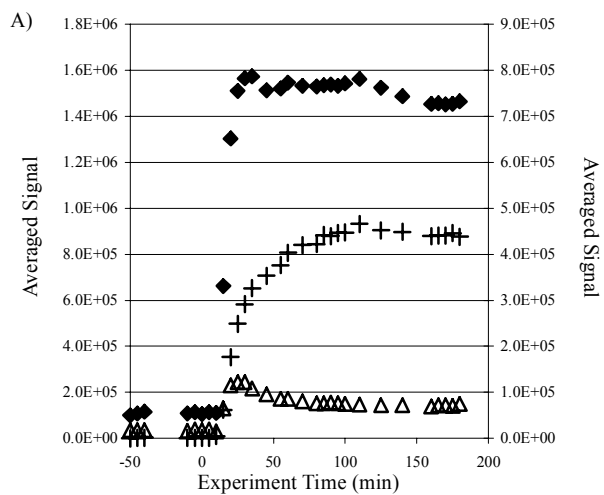


Fig. 9.

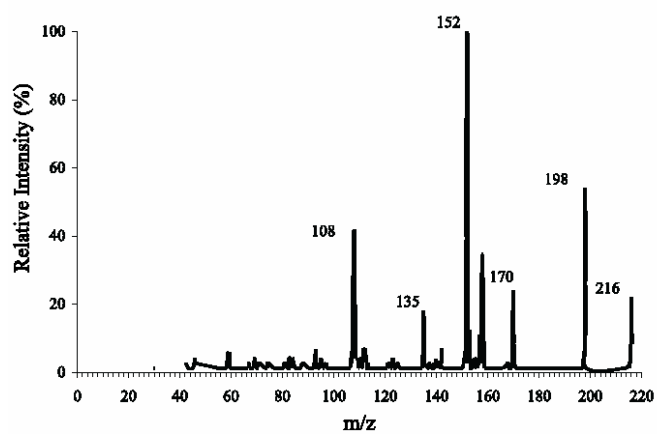


Fig. 10.

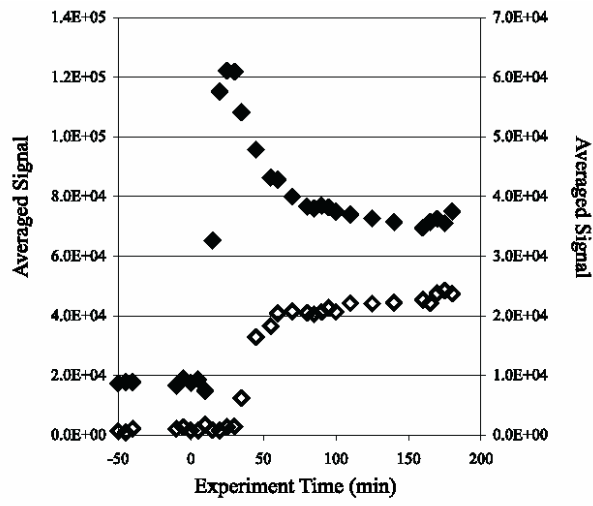


Fig. 11.